Journal of Reproduction and Development, Vol. 66, No 3, 2020

—Original Article—

Histone H3 methylation orchestrates transcriptional program in mouse spermatogenic cell line

Xiao-fei WANG[1)#], Qing TIAN[1)#], Wei-bing QIN[2) #], Ying YIN[3)], Ling ZENG[1)], Yun-ge TANG[2)], Ping SU[1)] and Li-quan ZHOU[1)]

[1)]*Institute of Reproductive Health, Tongji Medical College, Huazhong University of Science and Technology, Hubei 430030, China*

[2)]*NHC Key Laboratory of Male Reproduction and Genetics, Family Planning Research Institute of Guangdong Province, Guangzhou 510600, China*

[3)]*School of Basic Medicine, Tongji Medical College, Huazhong University of Science and Technology, Hubei 430030, China*

Abstract. Changes in histone modifications always correlate with altered transcriptional activities of genes. Recent studies have shown that the mutation of certain lysine residues to methionine in the histone variant H3.3 can act as a valuable tool to reduce specific H3 methylation levels. In our study, we used the mouse spermatogenic cell line GC-2 as a model to generate cells stably expressing H3.3 K4, H3.3 K9, H3.3 K27, and H3.3 K36M. The expression of these H3.3 K-to-M mutants influenced the expression of different subsets of genes, and a total of 891 differentially expressed genes were identified through global gene expression profiling. Moreover, the H3.3 K-to-M transgenes, especially H3.3 K36M, impacted the expression of endogenous retrovirus ERVK. This study gives a global view of how different H3 modifications regulate transcriptomes in spermatogenic cell lines, and identifies potential targets of H3 modifications in male germ line.

Key words: H3.3, Histone methylation, Retrotransposon, Spermatogenic

(**J. Reprod. Dev. 66:** 223–230, 2020)

Covalent post-translational modifications of histones, such as methylation, acetylation, phosphorylation, and ubiquitination [1], and histone H3 lysine methylation are widely studied since they are always enriched in regulatory elements. The well-known methylated H3 lysine residues include K4, K9, K27, and K36. H3K4/36 methylation is associated with gene activation [2–4]. H3K9 methylation is associated with heterochromatin formation and gene silencing [5, 6], and H3K27 methylation is related to repression of developmental genes, X chromosome inactivation, and gene imprinting [7, 8].

Histone H3.3 is a highly conserved histone H3 variant which is involved in many important biological processes, such as cell fate control and reprogramming. It can be incorporated into chromatins independent of DNA replication [9], unlike the canonical histone H3 [10]. K-to-M mutants in histone H3.3 drive brain and bone cancers in children [11], and tumors containing the mutated histone exhibit an overall loss of specific histone methylation markers [12]. K-to-M mutants in histone H3.3 play dominant-negative roles to suppress specific histone H3 methylation and can be used as a valuable tool to investigate how specific histone H3 methylation regulates gene expression and cell identity. For example, this strategy was used to find that the ectopic expression of H3.3 K4M destabilized enhancer H3K4 methyltransferases and disturbed adipose tissue development [13]. Another study showed that overexpression of H3.3K4M before fertilization led to reduced zygotic genome activation in paternal pronucleus, resulting in developmental arrest [14].

To investigate specific roles of certain histone H3 lysine methylations in mouse germ cell line GC-2 (GC-2spd, transformation of freshly isolated mouse spermatocytes), we ectopically expressed H3.3 K4M, K9M, K27M, and K36M mutants in GC-2 cells individually, and analyzed changes in the transcriptome, including expression of endogenous retroviruses. We chose GC-2 monocultures representing spermatogenesis systems to simulate complex cellular processes including proliferation and differentiation of male germ cells [15–17]. The results showed that almost all mutants significantly affected the global transcriptional program but in different subsets of genes in GC-2 cells.

Received: October 28, 2019
Accepted: January 20, 2020
Advanced Epub: February 11, 2020

[#] X-f Wang, Q Tian and W-b Qin contributed equally to this work.
Correspondences: L-q Zhou (e-mail: zhouliquan@hust.edu.cn), P Su (e-mail: suping24@126.com), Y-g Tang (e-mail: tyg813@126.com)

Materials and Methods

Vector construction

The expression plasmid encoding wildtype Drosophila H3.3 cDNA was previously described [18]. Site-directed mutagenesis was performed to produce H3.3 K-to-M mutations. A piggyBac plasmid (Addgene, 110824) was used as backbone, which contained the piggyBac terminal repeat sequence (*PB-TRs*) and the Blasticidin B (BSD) selection marker. H3.3 WT or H3.3 KM mutants, together with

the T2A-mCherry-polyA fragment were cloned into the piggyBac backbone. The T2A element between the H3.3 mutants and mCherry allowed for examination of the H3.3 transgene expression through fluorescence intensity of mCherry.

Establishment of GC-2 cell lines stably expressing different H3.3 K-to-M mutants

The GC-2 cells were purchased from Zhong Yuan Biological Ltd which obtained the cell line from the American Type Culture Collection (ATCC). Vectors encoding H3.3 WT or H3.3 K-to-M mutants were co-transfected with a piggyBac transposase expression vector into GC-2 cells with Lipofectamine 2000 (Thermo Fisher Scientific, Waltham, MA, USA) in order to generate stably transgenic GC-2 cell lines. Stably transgenic cells were selected in the presence of 10 μg/ml BSD (YEASEN Biotech, Shanghai, China) for 2 weeks, followed by further scaling up. We confirmed that mCherry signal can be detected in all stably transfected cells.

RNA-seq analysis

We used Trizol (Thermo Fisher Scientific) to extract total RNA from 1–2 × 10^7 cells, and 2 mg of total RNA was used to prepare standard RNA-seq libraries (TruSeq RNA Sample Preparation Kit, Illumina, San Diego, CA, USA). Libraries were sequenced using the Illumina HiSeq 3000 platform. The raw reads were processed with Cutadapt v1.16 (https://cutadapt.readthedocs.io) to remove adapters and perform quality trimming with default parameters except for: quality-cutoff = 20, minimum-length = 20. The trimmed reads were mapped to the mouse genome (GENCODE release M23) using STAR (v2.5.1b) with default settings. The reads were counted in exons of the mouse genome (GENCODE release M23) using the STAR-quantMode GeneCounts setting. The differential expression of genes for all pairwise comparisons was assessed by DESeq2 v1.24.0 (https://bioconductor.org/packages/release/bioc/html/DESeq2.html) with internal normalization of reads to correct for library size and RNA composition bias. The differentially regulated genes in the DESeq2 analysis were defined as those with more than a two-fold increase or decrease with adjusted $P < 0.05$. Cufflinks (https://github.com/cole-trapnell-lab/cufflinks) was used to calculate the FPKM value. Venn diagrams were generated using online tools (http://bioinformatics.psb.ugent.be/webtools/Venn/).

Weighted Gene Co-expression Network Analysis (WGCNA)

Weighted gene co-expression networks were constructed using the WGCNA package in R. The top 5,163 genes with the highest variation and the genes with top 25% coefficient of variation were further divided into 13 modules using WGCNA and correlation of each module was calculated. The module-trait relationships were estimated using the correlation between the module eigengene and mutants/control treatments. Network visualization for each module was performed using the Cytoscape software version 3.7.1. The gene co-expression network is a scale-free weighted gene network with multiple nodes connected to different nodes via edges. Each node represents a gene, which is in turn connected to a number of different genes. The gene which is connected to a greater number of genes is denoted by a bigger size and is more important for its interaction with a large number of genes.

Quantitative RT-PCR (qRT-PCR)

Total RNA was extracted using Trizol (Invitrogen, Carlsbad, CA, USA) and reverse transcribed using random primers with the PrimeScript RT reagent kit (Takara, Kusatsu, Japan) and real-time quantitative PCR was performed using AceQ qPCR SYBR Green Master Mix (Vazyme, Nanjing, China) and a LightCycler (Roche Applied Science, Indianapolis, IN, USA) according to the manufacturer's instructions (95°C for 3 min and 40 cycles of 95 °C for 10 sec, annealing temperature of 58–62ºC for 30 sec, and 72°C for 30 sec, followed by 72°C for 1 min). The details of the primer sequences are summarized in Supplementary Table 1 (online only).

Western blotting

The proteins from GC-2 cells were extracted using RIPA solution (50 mM Tris-HCl, 1% SDS, 1% NP-40, 0.25% Na-deoxycholate, 150 mM NaCl, 1mM EDTA), and their concentrations were determined using the bicinchoninic acid protein assay kit (Thermo Scientific, Waltham, MA, USA). The proteins were denatured, separated on a 12% SDS-PAGE gel, and transferred to a nitrocellulose membrane. The blots were incubated with the anti-Histone H3K4/K9/K27/K36 trimethylation antibody (Abcam, Cambridge, UK) in Tris-buffered saline (TBS) containing 0.1% Tween-20 at 4°C, overnight. The following day, the blots were incubated with a goat anti-rabbit horseradish peroxidase immunoglobulin G (IgG) secondary antibody (Abcam) at 37°C for 2 h. The protein bands were detected using a chemiluminescence detection kit (Applygen Technologies, Beijing, China) on X-ray films and analyzed using the Quantity One software (Bio-Rad, Hercules, CA, USA).

Statistical analysis

Statistical analysis was performed by R.

Results

PiggyBac transposon mediated efficient and stable integration of histone H3.3 K-to-M mutants in GC-2 cells

Firstly, we constructed a PiggyBac vector expressing mCherry driven by a cytomegalovirus (CMV) promoter, and inserted genes encoding histones H3.3 WT, K4M, K9M, K27M, and K36M (Fig. 1A). We then transfected these vectors into GC-2 cells, and acquired transgenic cells with stable expression levels of H3.3 transgenes. Western blotting was performed to confirm that the expression of these H3.3 K-to-M mutants dramatically reduced trimethylation of corresponding lysine residues of histone H3 (Fig. 1B).

Overexpression of H3.3 K-to-M mutants disturbed transcriptome of GC-2 cells

RNA sequencing was performed to further analyze the transcriptome of stable cell lines expressing H3.3 WT, K4M, K9M, K27M, and K36M. Principal Component Analysis (PCA) was firstly employed to show that the expression of H3.3 K4M, K9M and K36M, but not H3.3 K27M, significantly changed cell identity (Fig. 2A). To determine the effect of K-to-M mutants on transcriptional program, we performed comparative transcriptome analysis, with GC-2 cells expressing H3.3 WT as control (Fig. 2B). A total of 55,450 genes were analyzed, and 891 genes were differentially expressed

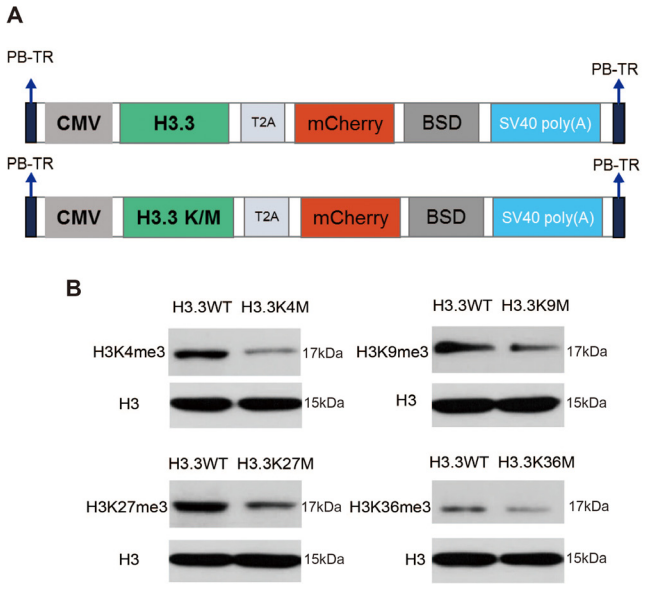

Fig. 1. PiggyBac transposon vectors that stably expressed H3.3 K-to-M mutants. (A) Schematic representation of the piggyBac transposon vectors used in this study. PB-TR, piggyBac terminal repeat elements; CMV, CMV promoter. (B) Western blot indicated that histone H3 trimethylation specifically altered in individual cells overexpressing histone H3.3 WT/KM transgenes.

in the 4 groups with the cut-off value to be two-fold the difference (Benjamini–Hochberg adjusted P-value < 0.05).

An MA plot was also used to visualize differential gene expression (Fig. 3A=3D). We observed that overexpression of H3.3 K4M led to downregulation of 252 genes and upregulation of 107 genes, implying that H3K4 methylation is mainly involved in gene activation (Fig. 3A). In contrast, more genes were upregulated in H3.3 K9M (164 *vs*. 43 genes), K27M (185 *vs*. 46 genes), and K36M (275 *vs*. 44 genes)-overexpressed cells, showing that methylation of these lysine residues mainly participates in gene silencing (Fig. 3B–3D).

We also performed GO analysis on misregulated genes in cells expressing H3.3 K4M, K9M, K27M, and K36M and found that distinct biological processes were enriched. This shows that methylation of different lysines in histone H3 regulates different biological events and plays different roles (Supplementary Fig. 1: online only).

H3K4/9/27/36 methylation regulated different subsets of genes

In order to identify co-regulated targets of different H3.3 K-to-M mutants, we compared the misregulated genes in cells expressing H3.3 K4M, K9M, K27M, and K36M. In general, the four groups have quite different misregulated genes, indicating that methylation of these lysine residues plays distinct roles in gene regulation (Fig. 4A). For example, when we analyzed the misregulated genes in H3.3 K4M and K9M groups, we identified that the downregulation gene list of H3.3 K4M group (252 genes) and the upregulation gene

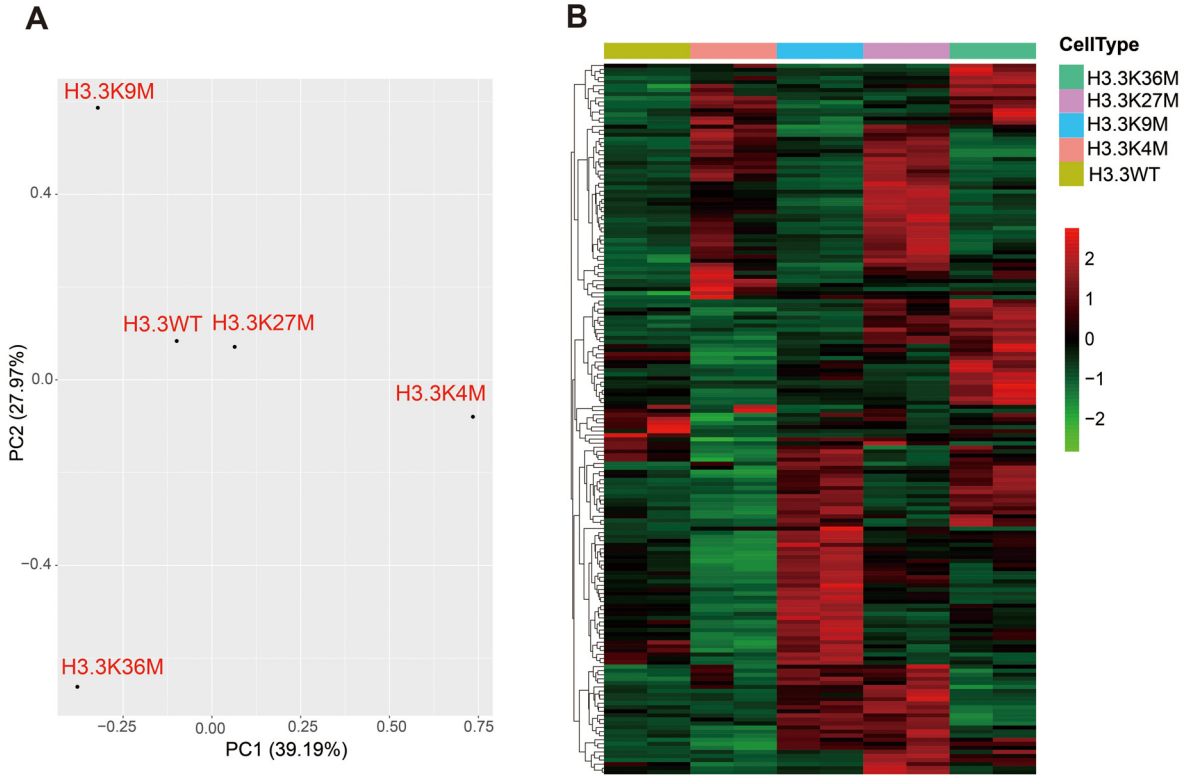

Fig. 2. Overexpression of H3.3 K-to-M mutants affected transcriptome of GC-2 cells. (A) PCA result shows that expression of H3.3 K4M, K9M and K36M, but not K27M, changed cell identity significantly. (B) Heatmap illustrates expression of all differentially expressed genes (more than 2-fold change; P < 0.05).

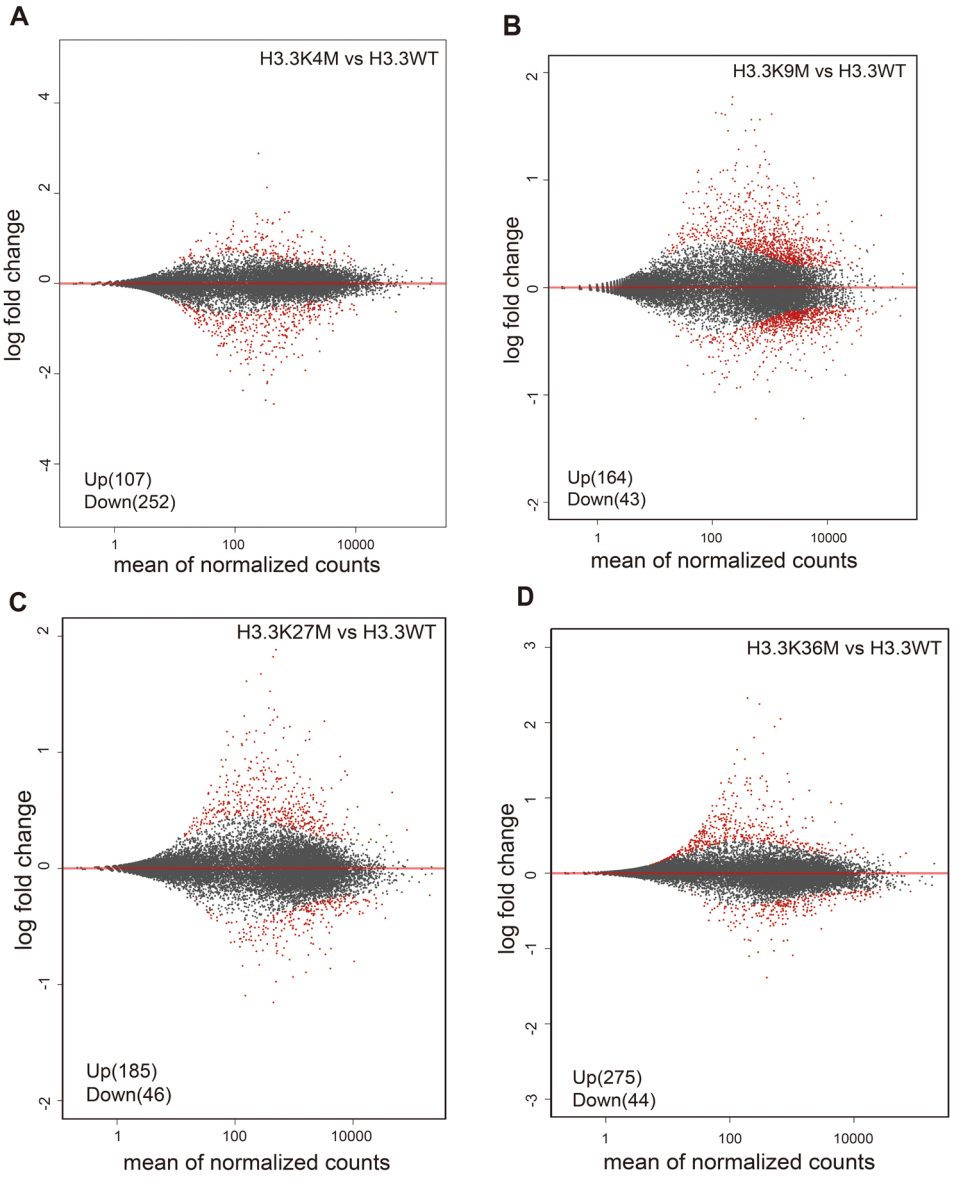

Fig. 3. MA plot visualizes up- and down-regulated genes after H3.3 K-to-M mutants overexpression. (A) H3.3K4M, (B) H3.3K9M, (C) H3.3K27M and (D) H3.3K36M. All differentially expressed genes are indicated in red.

list of H3.3 K9M group (164 genes) shared only 25 overlapped genes (Supplementary Fig. 2: online only). As expected, the H3.3 K4M and K9M groups have almost no overlapped downregulated or upregulated genes. We randomly selected specific up-regulated or down-regulated genes at each mutation site for verification. The expressions of several genes (*Satb1, Neurl3, Sgsm1, Wnt7a, Aldh1a7, Trim34a, Msx1 and Id4*) were examined by qRT-PCR. As shown in Fig. 4B, the results of the qRT-PCR in H3.3 K-to-M mutants were consistent with the RNA-seq results.

Notably, two genes, *Acta2* and *Krt16*, were misregulated in all mutant groups. The expression levels of these two differentially expressed genes were also examined by qPCR (Fig. 4C). The protein encoded by *Acta2* belongs to the actin family, which is a highly conserved protein that plays an important role in cell viability, structure and integrity. *Krt16* encodes a protein which is a member of the keratin gene family. Keratin is an intermediate filament protein responsible for the structural integrity of epithelial cells. Transcriptome analysis shows that the expression of *Acta2* and *Krt16* varies considerably in different tissues (https://www.ncbi.nlm.nih.gov/gene/), indicating that their transcriptional activities are sensitive to epigenetic signals. The proteins encoded by both the genes are components of the cytoskeleton, indicating the importance of cytoskeleton in cell fate determination.

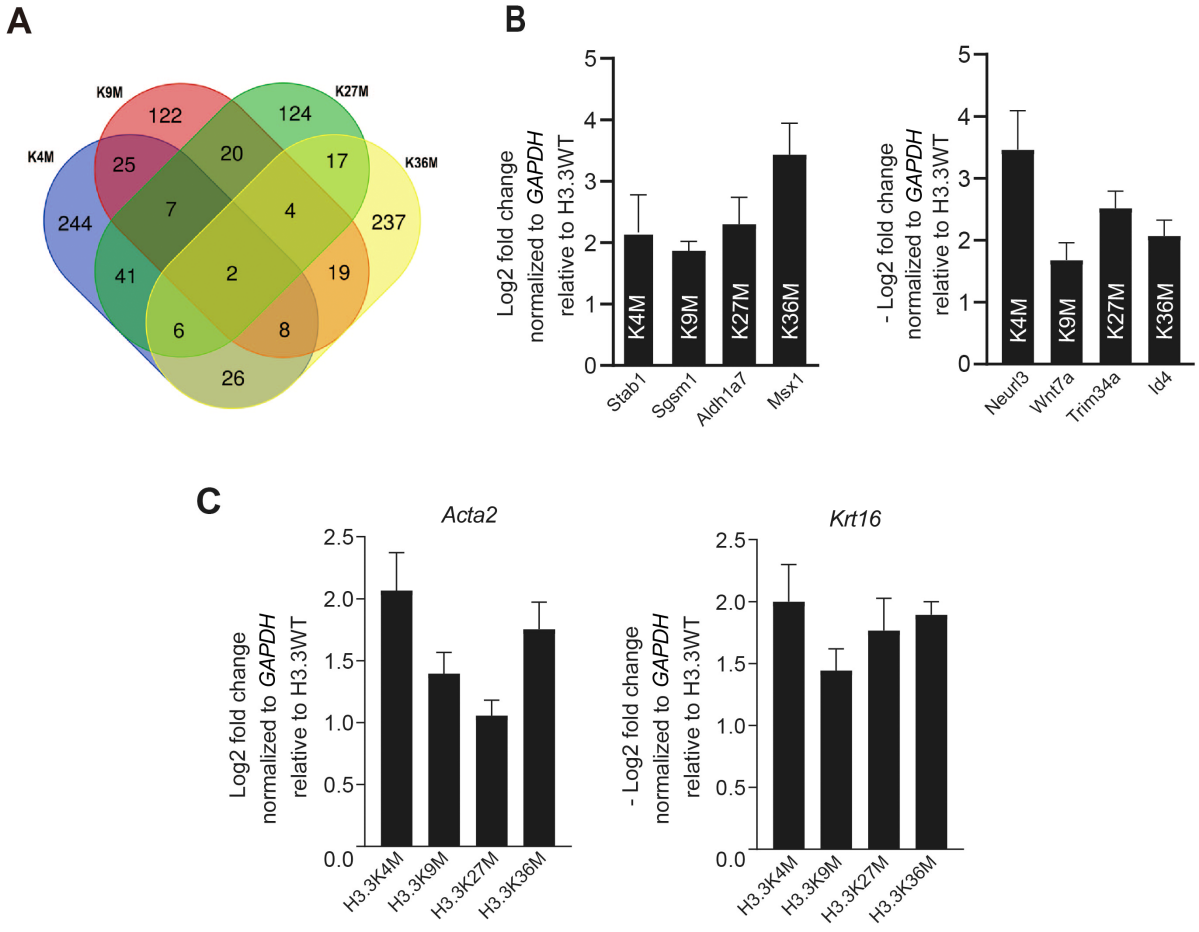

Fig. 4. Analysis of differentially expressed genes in GC-2 transcriptome by overexpression of H3.3 K-to-M mutants. (A) Venn diagram shows the number of co-regulated genes by H3.3 K4M, K9M, K27M and K36M transgenes. (B) The expression levels of eight differentially expressed genes in H3.3 K-to-M mutants were examined by qRT-PCR. (C) Relative expression of the 2 genes, *Acta2* and *Krt16*, both of which were misregulated in all groups.

Co-expression network analysis identified several hub genes regulating spermatogenesis

To explore the co-expression patterns among genes across cells expressing histone H3.3 K-to-M mutants, the weighted gene co-expression network analysis (WGCNA) was performed. A total of 5,163 genes with the highest variation were included in WGCNA analysis. The cluster dendrogram contained 13 co-expression modules, represented by different colors (Fig. 5A). The cluster dendrogram contained 13 co-expression modules, which are represented by brown, magenta, tan, green, black, purple, green yellow, dark grey, salmon, turquoise, dark turquoise, royal blue and grey color backgrounds (Fig. 5A). The numbers represent the Pearson correlation coefficients. The positive correlation is indicated in red while negative correlation is indicated in green. The number of genes in each module varies from 64 to 1151. In order to explore the functions of these modules, we selected those modules with the strongest correlation with H3.3 K-to-M mutant groups for further analysis (Fig. 5B). Four modules with strong correlation, including H3.3K4M-purple (r = 0.95), H3.3K9M-brown (r = 0.86), H3.3K27M-royal blue (r = 0.92) and H3.3K36M-green yellow (r = 0.87) were selected.

To further investigate the function of the co-expressed genes in the 4 modules, Cytoscape software was used for module analysis to find the hub genes. Eventually, we chose the top 30 hub genes with higher degree of connectivity. We found that a significant number of genes, such as *Foxo1*, *Tspyl1*, *Stag3*, *Stx2*, *Bmi1*, *Tdrp*, *Cdh2*, and *Eno4*, play crucial roles in reproduction, particularly male reproduction (Table 1). *Foxo1* is highly expressed in undifferentiated spermatogonia. Some studies have found that *Foxo1* controls all aspects of spermatogenesis, right from spermatogonial stem cell self-renewal to the initiation of spermatogenesis and meiosis [19]. *TSPY1* (Testis-specific protein, Y-encoded, 1) is involved in the regulation of spermatogenic efficiency via highly variable copy dosage, with dosage deficiency of the multicopy gene conferring an increased risk of spermatogenic failure [20]. *STAG3* encodes a meiotic-specific protein in the reproductive system, which is essential for the function of the meiotic adhesin complex. Sequence variations in *STAG3* have been reported to cause meiotic arrest in male and female mice, and premature ovarian failure in human females [21].

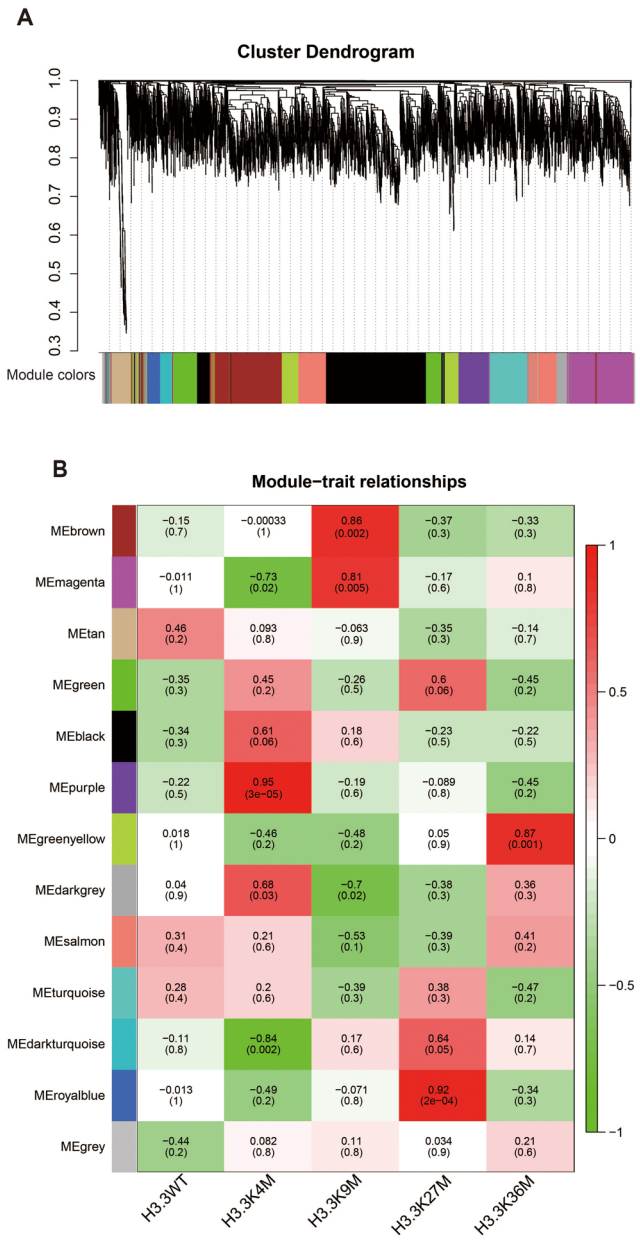

Fig. 5. Co-expression analysis of genes associated with different H3.3 K-to-M transgenes. (A) Gene distribution in the weighted gene co-expression network analysis (WGCNA) network which presents 13 gene co-expression modules. (B) Module-Trait relationships. The numbers represent the Pearson correlation coefficients. Positive correlation is indicated in red while negative correlation is indicated in green.

STX2 is required for maintenance of germ cell intercellular bridges during the meiotic prophase of spermatogenesis, and it contributes to intracellular and membrane localization of sulfoglycolipids. Mice deficient in *Stx2* exhibit spermatogenesis arrested at meiotic prophase, with the formation of multinucleated spermatocytes [22]. *Bmi1* is ubiquitously expressed in adult testes. Knockout of *Bmi1* in mice leads to male infertility with reduced testosterone syntheses, increased DNA damage, impaired germ cell differentiation and sperm malformation [23]. TDRP (Testis Development-Related Protein) interacts with *PRM2* and its deficiency contributes to low sperm motility [24]. N-cadherin coded by the *Cdh2* gene is important for maintenance of the testis cord structure and is required for the formation of steroidogenic cells. N-cadherin plays a major role in gonad differentiation, structuralization, and function [25]. Disruption of the spermatogenic cell-specific mouse enolase 4 (*Eno4*) gene results in defective sperm structure and male infertility [26]. Taken together, our list of hub genes, including a significant number of important regulators, control male reproduction.

Overexpression of H3.3 K-to-M mutants disrupted silencing of ERVK retrotransposon

Retrotransposons are mobile genetic elements widely distributed in eukaryotic genomes. They cause recombination and mutations in genome, and play important roles in genome evolution and horizontal sequence transfer between species to shape the genomes of organisms. Retrotransposons are silenced in male germ cells and the related mechanisms are conserved and essential for male reproduction. *piRNAs* play critical roles in inhibiting their activation to maintain genome stability of male germ cells. Activation of retrotransposons in spermatogenic cells results in developmental arrest at different stages of spermatogenesis and failure to produce spermatozoa.

Here, we examined the expression changes of retrotransposons in GC-2 cells expressing H3.3 K-to-M mutants (Table 2). Interestingly, only ERVK, which belongs to LTR retrotransposon, was misregulated, showing that ERVK is the most sensitive retrotransposon when histone H3 lysine methylation is inhibited.

According to our data, histone H3.3 K27M had no significant influence on retrotransposon expression, while histone H3.3K36M expression had the most significant impact on retrotransposon reactivation. Intracisternal A-particle (IAP) belongs to ERV retrotransposons and is active in mice. Notably, IAP elements were activated when H3.3 K4M, K9M, and K36M were expressed. Taken together, our results showed that H3K4/9/36 methylation is important for retrotransposon silencing and genome stability.

Discussion

N-terminal lysine residues of histone H3 can be methylated through histone methyltransferases. Genome-wide profiling of histone modifications demonstrates that individual lysine methylation of histone H3 is strongly correlated with distinct transcriptional events regulating gene activation/repression and chromatin structure [27], and maintenance of proper level and distribution of specific histone methylation is essential for physiological processes in organisms. Abnormal histone modifications may lead to aberrant cell proliferation, cell apoptosis, and cancer [28].

Previous studies have shown that overexpression of histone H3.3 K-to-M mutants cause significant decrease in global H3 methylation at specific lysine residues, and this change disturbed the expression of many genes, ultimately affecting the development of the organism and leading to formation of cancer [11, 12]. Therefore, histone H3.3 K-to-M mutants are useful tools to study how specific H3 modifica-

Table 1. Important HUB genes for reproduction identified by weighted gene co-expression network analysis (WGCNA)

Module	Hub gene	Function	References
H33K4M purple	*Foxo1*	Maintaining SSC and initiating spermatogenesis	[19]
	Tspyl1	Regulation of spermatogenic efficiency	[20]
H33K9M brown	*Stag3*	Encoding for a meiosis-specific protein	[21]
	Stx2	Maintaining intercellular bridges of spermatocytes	[22]
H33K27M royalblue	*Bmi1*	Promoting cell cycle progression	[23]
	Tdrp	Encoding testis development-related protein	[24]
H33K36M greenyellow	*Cdh2*	Maintenance of testis cord structure and formation of steroidogenic cells	[25]
	Eno4	Assembly fibrous sheath normal and provided the enolase activity in sperm	[26]

Table 2. Retrotransposons affected by overexpression of H3.3 K-to-M mutations

	Total	Class	Name	log2FoldChange	padj
H33K4M	2	LTR: ERVK	IAP-d-int	1.662222534	4.48E-09
			MMERVK10D3_I-int	1.493018803	0.000273123
H33K9M	3	LTR: ERVK	IAP-d-int	1.640381507	1.50E-18
			MMERVK10D3_I-int	1.551878854	7.41E-15
			RLTR10D2	1.651761573	0.038077465
H33K27M	1	LTR: ERVK	RNERVK23-int	–0.6936	0.023124081
H33K36M	7	LTR: ERVK	MMERVK10D3_I-int	3.615139152	1.90E-149
			IAP-d-int	2.583408611	2.61E-57
			RLTR10D2	3.145393451	5.22E-12
			RLTR45-int	1.566366399	3.40E-06
			IAPLTR3-int	1.905315171	7.96682E-05
			RLTRETN_Mm	1.307904893	0.000844666
			IAP1-MM_I-int	1.418439409	0.001856773

tions are involved in different biological processes. Residue-specific histone methylation is generally associated with gene activation or suppression. To investigate the role of methylation of certain histone H3 lysine residues in the reproductive system, we overexpressed several H3.3 K-to-M mutants and found that these mutants did inhibit corresponding H3 modifications in the transfected cells, and changed the expression of multiple genes. In our study, H3.3 K4M, K9M, K27M, and K36M significantly affected the expression of 359, 207, 231, and 319 genes, respectively.

By analyzing differentially expressed genes in GC-2 cells, we found that the overexpression of different H3.3 K-to-M mutants led to misregulation of different subsets of genes, indicating diverse regulatory patterns of different biological processes and complexity of transcriptional network. Interestingly, two genes, Acta2 and Krt16, were both misregulated when H3.3 K4M, K9M, K27M, or K36M was overexpressed. Both these genes are important components of the cytoskeleton, suggesting that the cytoskeleton plays a significant role in cell fate control. We also performed a weighted gene co-expression network analysis on our sequencing results, looked for modules that are synergistically expressed, and explored the hub genes in the regulatory network. We found that many hub genes such as *Foxo1*, *Tspyl1*, *Stag3*, *Stx2*, *Bmi1*, *Tdrp*, *Cdh2*, and *Eno4* are involved in male reproduction. Finally, disrupted silencing of the retrotransposon ERVK, including the IAP element, was detected when H3.3 K-to-M mutants were overexpressed. Among different histone methylations, H3K9me3 is well-known to silence endogenous retroviruses. Previous reports indicate that the H3K9 methyltransferase ESET (also known as SETDB1) catalyzes H3K9me3 for silencing endogenous retroviruses in mouse ES cells [25, 29].

Changes in histone methylation influence gene expression and biological processes in cells. Aberrant modification of histone methylation may impact development and stress responses, and can cause cancer and other diseases [30]. Our study used a male germ cell line to demonstrate that methylation of different lysine residues significantly alters the expression of different genes which are involved in various cellular processes, suggesting that methylation of diverse lysine residues in histones is involved in distinct developmental events in male germ cells. Therefore, it will be interesting to further explore the role of the above histone methylation through transgenic mouse models. Meanwhile, our results of high-throughput sequencing data produced valuable resources to link individual genes to different histone methylation activities, providing potential gene candidates for other related studies involving the disruption of histone H3 methylation.

Conflict of interest: The authors declare no conflict of interest.

Acknowledgments

This research was supported by the National Key R&D Program of China (2018YFC1004502, 2018YFC1004001), the Foundation of NHC Key Laboratory of Male Reproduction and Genetics (KF201804), and the National Natural Science Foundation of China (NSFC 31771661).

References

1. **Allfrey VG, Faulkner R, Mirsky AE.** Acetylation and methylation of histones and their possible role in the regulation of RNA synthesis. *Proc Natl Acad Sci USA* 1964; **51**: 786–794. [Medline] [CrossRef]
2. **Santos-Rosa H, Schneider R, Bannister AJ, Sherriff J, Bernstein BE, Emre NC, Schreiber SL, Mellor J, Kouzarides T.** Active genes are tri-methylated at K4 of histone H3. *Nature* 2002; **419**: 407–411. [Medline] [CrossRef]
3. **Krogan NJ, Kim M, Tong A, Golshani A, Cagney G, Canadien V, Richards DP, Beattie BK, Emili A, Boone C, Shilatifard A, Buratowski S, Greenblatt J.** Methylation of histone H3 by Set2 in Saccharomyces cerevisiae is linked to transcriptional elongation by RNA polymerase II. *Mol Cell Biol* 2003; **23**: 4207–4218. [Medline] [CrossRef]
4. **Morillon A, Karabetsou N, Nair A, Mellor J.** Dynamic lysine methylation on histone H3 defines the regulatory phase of gene transcription. *Mol Cell* 2005; **18**: 723–734. [Medline] [CrossRef]
5. **Goll MG, Bestor TH.** Histone modification and replacement in chromatin activation. *Genes Dev* 2002; **16**: 1739–1742. [Medline] [CrossRef]
6. **Schultz DC, Ayyanathan K, Negorev D, Maul GG, Rauscher FJ 3rd.** SETDB1: a novel KAP-1-associated histone H3, lysine 9-specific methyltransferase that contributes to HP1-mediated silencing of euchromatic genes by KRAB zinc-finger proteins. *Genes Dev* 2002; **16**: 919–932. [Medline] [CrossRef]
7. **Ringrose L, Paro R.** Epigenetic regulation of cellular memory by the Polycomb and Trithorax group proteins. *Annu Rev Genet* 2004; **38**: 413–443. [Medline] [CrossRef]
8. **Wang L, Brown JL, Cao R, Zhang Y, Kassis JA, Jones RS.** Hierarchical recruitment of polycomb group silencing complexes. *Mol Cell* 2004; **14**: 637–646. [Medline] [CrossRef]
9. **Krimer DB, Cheng G, Skoultchi AI.** Induction of H3.3 replacement histone mRNAs during the precommitment period of murine erythroleukemia cell differentiation. *Nucleic Acids Res* 1993; **21**: 2873–2879. [Medline] [CrossRef]
10. **Frank D, Doenecke D, Albig W.** Differential expression of human replacement and cell cycle dependent H3 histone genes. *Gene* 2003; **312**: 135–143. [Medline] [CrossRef]
11. **Nacev BA, Feng L, Bagert JD, Lemiesz AE, Gao J, Soshnev AA, Kundra R, Schultz N, Muir TW, Allis CD.** The expanding landscape of 'oncohistone' mutations in human cancers. *Nature* 2019; **567**: 473–478. [Medline] [CrossRef]
12. **Chan KM, Fang D, Gan H, Hashizume R, Yu C, Schroeder M, Gupta N, Mueller S, James CD, Jenkins R, Sarkaria J, Zhang Z.** The histone H3.3K27M mutation in pediatric glioma reprograms H3K27 methylation and gene expression. *Genes Dev* 2013; **27**: 985–990. [Medline] [CrossRef]
13. **Jang Y, Broun A, Wang C, Park YK, Zhuang L, Lee JE, Froimchuk E, Liu C, Ge K.** H3.3K4M destabilizes enhancer H3K4 methyltransferases MLL3/MLL4 and impairs adipose tissue development. *Nucleic Acids Res* 2019; **47**: 607–620. [Medline] [CrossRef]
14. **Aoshima K, Inoue E, Sawa H, Okada Y.** Paternal H3K4 methylation is required for minor zygotic gene activation and early mouse embryonic development. *EMBO Rep* 2015; **16**: 803–812. [Medline] [CrossRef]
15. **Solek P, Majchrowicz L, Bloniarz D, Krotoszynska E, Koziorowski M.** Pulsed or continuous electromagnetic field induce p53/p21-mediated apoptotic signaling pathway in mouse spermatogenic cells in vitro and thus may affect male fertility. *Toxicology* 2017; **382**: 84–92. [Medline] [CrossRef]
16. **Sun J, Wang J, He L, Lin Y, Wu J.** Knockdown of polycomb-group RING finger 6 modulates mouse male germ cell differentiation in vitro. *Cell Physiol Biochem* 2015; **35**: 339–352. [Medline] [CrossRef]
17. **Zhou J, Qian CY, Tong RQ, Wang B, Chen XL, Zhuang YY, Xia F, He Q, Lv JX.** Hypoxia induces apoptosis of mouse spermatocyte GC-2 cells through activation of autophagy. *Cell Biol Int* 2018; **42**: 1124–1131. [Medline] [CrossRef]
18. **Zhou L, Baibakov B, Canagarajah B, Xiong B, Dean J.** Genetic mosaics and time-lapse imaging identify functions of histone H3.3 residues in mouse oocytes and embryos. *Development* 2017; **144**: 519–528. [Medline] [CrossRef]
19. **Goertz MJ, Wu Z, Gallardo TD, Hamra FK, Castrillon DH.** Foxo1 is required in mouse spermatogonial stem cells for their maintenance and the initiation of spermatogenesis. *J Clin Invest* 2011; **121**: 3456–3466. [Medline] [CrossRef]
20. **Yang X, Leng X, Tu W, Liu Y, Xu J, Pei X, Ma Y, Yang D, Yang Y.** Spermatogenic phenotype of testis-specific protein, Y-encoded, 1 (TSPY1) dosage deficiency is independent of variations in TSPY-like 1 (TSPYL1) and TSPY-like 5 (TSPYL5): a case-control study in a Han Chinese population. *Reprod Fertil Dev* 2018; **30**: 555–562. [Medline] [CrossRef]
21. **van der Bijl N, Röpke A, Biswas U, Wöste M, Jessberger R, Kliesch S, Friedrich C, Tüttelmann F.** Mutations in the stromal antigen 3 (STAG3) gene cause male infertility due to meiotic arrest. *Hum Reprod* 2019; **34**: 2112–2119. [Medline]
22. **Nakamura S, Kobori Y, Ueda Y, Tanaka Y, Ishikawa H, Yoshida A, Katsumi M, Saito K, Nakamura A, Ogata T, Okada H, Nakai H, Miyado M, Fukami M.** STX2 is a causative gene for nonobstructive azoospermia. *Hum Mutat* 2018; **39**: 830–833. [Medline] [CrossRef]
23. **Dai X, Zhang Q, Yu Z, Sun W, Wang R, Miao D.** *Bmi1* deficient mice exhibit male infertility. *Int J Biol Sci* 2018; **14**: 358–368. [Medline] [CrossRef]
24. **Mao S, Wu F, Cao X, He M, Liu N, Wu H, Yang Z, Ding Q, Wang X.** TDRP deficiency contributes to low sperm motility and is a potential risk factor for male infertility. *Am J Transl Res* 2016; **8**: 177–187. [Medline]
25. **Piprek RP, Kolasa M, Podkowa D, Kloc M, Kubiak JZ.** N-Cadherin is critical for the survival of germ cells, the formation of steroidogenic cells, and the architecture of developing mouse gonads. *Cells* 2019; **8**: 8. [Medline] [CrossRef]
26. **Nakamura N, Dai Q, Williams J, Goulding EH, Willis WD, Brown PR, Eddy EM.** Disruption of a spermatogenic cell-specific mouse enolase 4 (eno4) gene causes sperm structural defects and male infertility. *Biol Reprod* 2013; **88**: 90. [Medline] [CrossRef]
27. **Cheng X.** Structural and functional coordination of DNA and histone methylation. *Cold Spring Harb Perspect Biol* 2014; **6**: 6. [Medline] [CrossRef]
28. **Song Y, Wu F, Wu J.** Targeting histone methylation for cancer therapy: enzymes, inhibitors, biological activity and perspectives. *J Hematol Oncol* 2016; **9**: 49. [Medline] [CrossRef]
29. **Matsui T, Leung D, Miyashita H, Maksakova IA, Miyachi H, Kimura H, Tachibana M, Lorincz MC, Shinkai Y.** Proviral silencing in embryonic stem cells requires the histone methyltransferase ESET. *Nature* 2010; **464**: 927–931. [Medline] [CrossRef]
30. **McCabe MT, Mohammad HP, Barbash O, Kruger RG.** Targeting histone methylation in cancer. *Cancer J* 2017; **23**: 292–301. [Medline] [CrossRef]